Biometric recognition via fixation density maps

Ioannis Rigas[*a], Oleg V. Komogortsev[a]
[a]Texas State University, 601 University Drive, San Marcos, TX 78666

ABSTRACT

This work introduces and evaluates a novel eye movement-driven biometric approach that employs eye fixation density maps for person identification. The proposed feature offers a dynamic representation of the biometric identity, storing rich information regarding the behavioral and physical eye movement characteristics of the individuals. The innate ability of fixation density maps to capture the spatial layout of the eye movements in conjunction with their probabilistic nature makes them a particularly suitable option as an eye movement biometrical trait in cases when free-viewing stimuli is presented. In order to demonstrate the effectiveness of the proposed approach, the method is evaluated on three different datasets containing a wide gamut of stimuli types, such as static images, video and text segments. The obtained results indicate a minimum EER (Equal Error Rate) of 18.3 %, revealing the perspectives on the utilization of fixation density maps as an enhancing biometrical cue during identification scenarios in dynamic visual environments.

Keywords: eye movement biometrics, behavioral characteristics, fixation density maps

1. INTRODUCTION

The research of eye movements in the field of biometrical identification has emerged the last few years with the realization that they can offer a plethora of physical and behavioral characteristics that can be extracted from the human subjects. Eye movements exhibit many of the favorable attributes that are frequently met in other behavioral approaches in biometrics, as for example the fundamental resistance in replication and the capability of unobtrusive sample recording. Furthermore, communication through the eyes seems as the most natural way for human-computer interaction for the upcoming augmented reality technologies that involve touch-less environments (e.g. the Google Glass project [1]). Compared to the other sources of behavioral features, eye movements present another advantageous characteristic which emanates from the fact that they are recorded from the face region. As a result, although eye movement traits can be used in standalone mode, they may also be easily incorporated in a multimodal framework (e.g. [2]), which would include other methods that also extract features from the face region, as for example iris recognition, periocular biometrics and face identification.

Until now, very few works have explored different biometric features that can be extracted from the eye movements, with the first work in [3] investigating the spectral attributes of eye movements by using the Cepstrum transform. In [4] several static and dynamic features have been inspected, such as the distance between the eyes, the pupil diameter and the gaze velocity, in a processing scenario that included the application of Fast Fourier Transform (FFT) and Principal Component Analysis (PCA) on the signals. An approach that adopted techniques from the field of voice recognition was suggested in [5], aiming to evaluate eye movements in a task independent visual scenario. In [6], a model based on anatomical characteristics of the eye and neural control signals, i.e. the Oculomotor Plant Characteristic (OPC), was presented for the description of eye movements. A graph based framework was proposed in [7], focusing on the comparison of eye movement characteristics mainly in the spatial domain. Most recently, in [8] the Complex Eye Movement Patterns (CEM-P) were presented as a representation model of the underlying brain strategies taking place during the guidance of eyes and the possible idiosyncratic features imprinted on them were explored. Finally, the research conducted in [9] examined the extraction of potential unique characteristics from the corrective oculomotor movements and their applicability in the field of biometrics.

In this paper, we propose a novel approach for evaluating the similarity of fixation signatures, formed during the observation of a stimulus in free-viewing conditions. Most of the research work that has been previously conducted concerns features of the time/spectral domain. Our objective is to tackle the case of spatial domain characteristics, suggesting a representation that may enfold physical and behavioral properties of the visual scanpath on the stimulus plane.

*rigas@txstate.edu; phone: 1 512 245-3409

Our inspiration for the proposed biometric feature was triggered from the work that is conducted in the research field of visual saliency. Visual saliency and attention modeling have drawn much scientific interest, especially in the field of computer vision [10], [11], [12], where saliency maps are constructed using low-level visual information in order to facilitate scene interpretation and content understanding. In an analogous manner, our proposed approach rather than using the image content information itself for the construction of a saliency map, it directly employs the fixation samples recorded from human individuals during the inspection of visual content for the formation of a fixation density map. Subsequently, by utilizing methods developed for the comparison of low-level content saliency maps we evaluate the similarity of the constructed personalized maps and perform identification based on the eye movement traits of each person.

2. FIXATION DENSITY MAPS

2.1 Formation of Fixation density maps

The basic element that will serve as a biometric feature in the proposed scheme is the fixation density map. Our motivation for the utilization of fixation density maps for the comparison of eye movements may be fully comprehended considering their following attributes: a) Fixation density maps efficiently capture spatial layout of eye movements. b) Construction and comparison of fixation density maps can be easily conducted by the established probabilistic methods for low-level saliency maps. c) Apart from the spatial features, implicit information about the duration of fixations may also be extracted from the magnitude of density values at various image regions.

The basic scheme that was implemented for the acquisition and processing of eye movement signals and the construction of biometrical templates can be inspected in Figure 1.

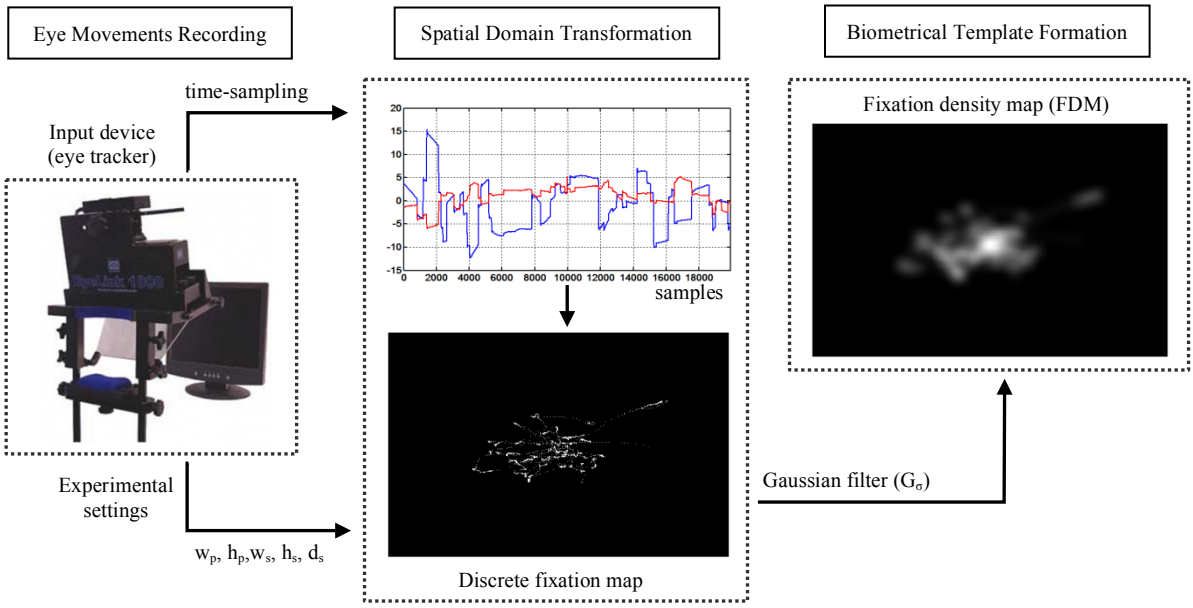

Figure 1. Overview of the proposed scheme for the transformation of an eye movement recording into a biometrical template.

In every enrollment, the eye movements made by each subject are recorded with an eye tracking device, providing a raw eye movement time-sampled signal of the horizontal and vertical position of the eye with respect to the presented stimuli on a computer screen. The transformation of a raw eye movement sequence into a fixation density map follows several processing steps. Initially, we need to obtain a proper correspondence between the recorded eye movements and the stimulus (image or video sequence) for which these eye movements have been generated. Since most of the eye tracking devices provide eye trajectory recordings in terms of distance (Δx_i, Δy_i) or visual angle (θx_i, θy_i) from the center of the presented stimulus, we have to use the recording parameters during a particular experiment in order to transform the eye

movement signal from the temporal domain into the spatial domain (px_i, py_i - pixel coordinates). These parameters are the resolution of the presented images (h_p x w_p), the dimensions of the screen (h_s x w_s) and the distance between the viewer and the screen (d_s). After the acquisition of these settings the transformation may occur with the use of equations (1) and (2):

$$px_i = \left(w_s/2\right) + \left(w_s/w_p\right) \cdot \Delta x_i \;, \quad \Delta x_i = \tan(\theta x_i \cdot \pi / 180^0) \cdot d_s \tag{1}$$

$$py_i = \left(h_s/2\right) + \left(h_s/h_p\right) \cdot \Delta y_i \;, \quad \Delta y_i = \tan(\theta y_i \cdot \pi / 180^0) \cdot d_s \tag{2}$$

Using the calculated pixel coordinates a discrete fixation map can be constructed as:

Discrete fixation map: $$\mathrm{fMap}(px, py) = \sum_{i=1}^{K} \delta((px, py) - (px_i, py_i)) \tag{3}$$

where K is the number of fixation samples.

After this initial processing step we have generated a simple fixation map. This map itself is a collection of discrete samples that it is highly unlikely to be exactly replicated even by the same person due to within-subject behavioral variations, noises in the human visual system, and inaccuracies in the recording equipment. Consequently, the discrete fixation map needs to be further translated into a form that would represent the recorded fixation data in a probabilistic layout. This representation can be implemented with the application of a Gaussian kernel on the constructed discrete fixation map, transforming it thus into a fixation density map:

Fixation density map (FDM): $$\mathrm{FDM}(px, py) = \mathrm{fMap}(px, py) * G_\sigma(px, py) \tag{4}$$

An important parameter that is involved during the construction of the density map is the standard deviation (σ) of the Gaussian kernel. An appropriate selection of this parameter is crucial because a large value of σ could result in an incorrect representation of the visual scanpath, whereas a too small value would not provide the probabilistic framework for the samples comparison. Although the precise influence of this parameter may depend on the exact settings of the recording experiment, the qualitative effect of varying the parameter σ of the Gaussian kernel on the fixation map may be observed in Figure 2. Furthermore, the quantitative impact of the value of this parameter on the identification rates for the employed experimental datasets is explored during the evaluation section (Section 3.2).

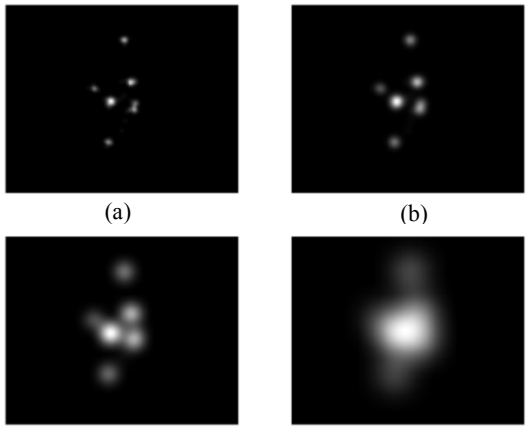

Figure 2. Visual inspection of the influence of the Gaussian kernel's σ value on the fixation density maps. (a) σ = 0.008, (b) σ = 0.016, (c) σ = 0.032 and (d) σ = 0.064 (σ normalized in map's width).

2.2 Comparison of Fixation Density Maps

In order to estimate the similarity of the extracted biometric features we will employ and evaluate two different comparison methods. These methods have been assessed in the field of low-level visual saliency and provide a framework in which the inspection of activation on two activation maps may occur in a probabilistic manner.

i) Similarity metric

This metric has been proposed in [13] for the comparison of saliency maps during modeling of visual attention. We will incorporate the Similarity metric in our particular scenario that concerns biometrical template matching. The Similarity metric provides a simple way for measuring how similar two distributions are (here the distributions are represented by the fixation density maps). The algorithmic path for the comparison of two fixation maps initiates by scaling each distribution to sum to one. In the sequence a similarity measure can be calculated by summing the minimum values at each point for the two distributions under consideration:

$$\text{Similarity metric}(P,Q) = \sum_{i,j} \min\left(P_{i,j}, Q_{i,j}\right) \tag{5}$$

where $\sum_{i,j} P_{i,j} = \sum_{i,j} Q_{i,j} = 1$. In Figure 3 we may observe the results of calculating the Similarity metric in two distinct cases. On the top (Figure 3a) we can see two maps that correspond at the same image and derive from the same subject whereas on the bottom (Figure 3b) the maps correspond at the same image and derive from different subjects. It can be easily verified that in the first case the compared maps share more similar parts, something that is also reflected by their Similarity metric which has a relatively higher value of 0.69 than in the second case which is 0.49.

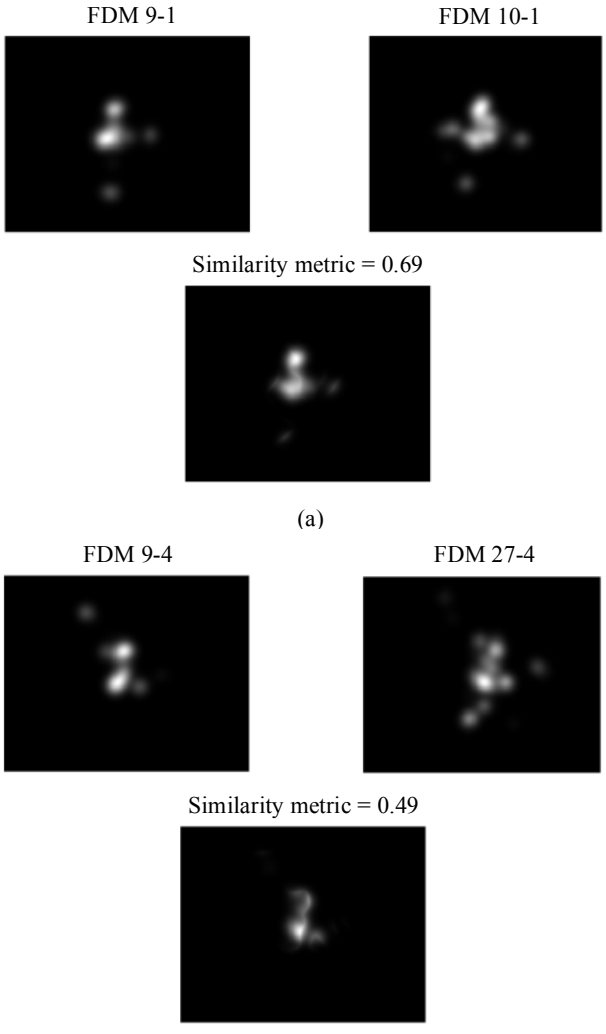

Figure 3. Computation of Similarity metric for pairs of fixation density maps coming (a) from the same individual and (b) from different individuals.

ii) Kullback-Leibler divergence

The divergence of Kullback-Leibler [14] provides an alternative measure for the expression of the overall dissimilarity between two probability density functions. Let us define two discrete distributions P and Q with probability density functions $p_{i,j}$ and $q_{i,j}$, then the KL-divergence between P, Q can be given by the relative entropy of Q with respect to P:

$$KL(P,Q) = \sum_{i,j} q_{i,j} \log\left(\frac{q_{i,j}}{p_{i,j}}\right) \tag{6}$$

with the restrictions that $p_{i,j}$ and $q_{i,j}$ sum to 1 and $p_{i,j} > 0$ for any i,j such that $q_{i,j} > 0$.

In our current scenario the KL-divergence is employed to measure the dissimilarity of the activation distribution (density values) on the fixation density maps. KL-divergence lacks of a well-defined upper bound and it is a non-symmetric measure, generating thus pseudo-Euclidean dissimilarity matrices during the comparison procedure. The idea of working in the dissimilarity space has been suggested in the past for addressing the problem of classification in the presence of non-Euclidean matrices [15], [16]. The procedure that is followed in the present work for conducting the classification stage in the dissimilarity space by using the computed KL-divergences is formulated as follows:

Let us denote D the full N x N matrix containing the KL-divergence values calculated from N different samples. If D_L is the lower triangle of the full matrix, then we can use these values in order to construct a symmetric matrix (D_S) as:

$$D_S = D_L + \left(D_L\right)^T - \mathrm{diag}\left(D\right) \tag{7}$$

Considering each row of the new matrix as a feature of the dissimilarity space we can subsequently calculate the Euclidean distances between the features, resulting thus in an Euclidean distance matrix (D_{Final}) which is symmetrical and has a well-defined upper bound:

$$D_{Final}\left(i,j\right) = \frac{D_{Eucl}\left(i,j\right)}{\max_{i,j}\left(D_{Eucl}\right)}, \quad i,j = 1,\ldots,N \tag{8}$$

where $D_{Eucl} = \mathrm{Euclidean}\left(D_S, \left(D_S\right)^T\right)$. This matrix, which in turn is transformed into a similarity matrix, can be used during the classification stage in order to evaluate the KL-divergence as a measure for the comparison of the fixation density maps generated by different individuals.

3. EXPERIMENTAL EVALUATION

3.1 Experimental Datasets

Three eye movement datasets are employed in order to evaluate the degree to which the proposed scheme is capable of effectively capturing the idiosyncrasies in the fixation distributions of individuals. One of them has been already used in the past for the evaluation of graph-based techniques in the field of eye movement biometrical identification whereas the other two are originally presented in the current paper. The utilized datasets allow for a thorough inspection of the examined algorithms behavior since they have been recorded under a variety of experimental scenarios, including different types of visual stimulus (faces, video sequences, text) and the employment of recording devices of different specifications. The strongest reason for the employment of these specific datasets though, lies in two remarkable characteristics they possess. First, they provide repetitive recordings for the exact same visual stimulus (images, video or text), offering a common ground on which the fixation distributions coming from the same and from different subjects may be compared. Furthermore, in contrast to more simple types of visual stimuli, e.g. a jumping point of light [6], the stimuli in these sets allow for free-viewing conditions, a feature that essentially facilitates the extraction of spatial features.

Faces dataset

The first dataset that is employed for our experiments has been assembled in [7] and the stimulus that was used consisted of human faces. The dataset was recorded from 15 subjects (12 male / 3 female) aged in a range of 20 - 30. Although the

number of subjects in this dataset is relatively small, we included it during the evaluation procedure so that we can compare the performance of the proposed approach with another method that has been already tested for the comparison of eye movement features in the spatial domain. During the experiments, each subject viewed a sequence of 10 different face images while his/her eye movements were recorded and the experiment was repeated totally for 8 times (enrollments), forming a database of 120 recordings (with 10 sub-signals for each corresponding face image). The eye movements were captured with the Eye Tracker Toolbox 50 Hz of CRS (Cambridge Research Systems) with a spatial accuracy 0.125^0 - 025^0. In order to calculate the similarity between two samples coming from different enrollments, we pairwise compare the sub-signals that correspond at the same face images (same content spatial layout) and average the computed values over all ten images.

Text dataset

This dataset was recorded during a reading task experiment and contains samples from a considerably larger pool of 100 subjects (52 male / 48 female), ages 18 - 43 with an average age of 22 (SD = 3.86). A total of 2 recordings were collected from every person, resulting thus in a database consisting of 200 different samples. The recordings were performed using an EyeLink-II eye tracker [17] running at 1000 Hz, with vendor reported spatial accuracy 0.5^0 and a measured average calibration accuracy of 0.47^0 (SD = 0.17^0). The average data validity was 94.86% (SD = 5.87%). The text stimulus consists of a collection of excerpts from the poem of Lewis Carroll 'The Hunting of the Snark' and it was presented in a flat computer screen in a distance of 550 millimeters from the subject eyes, with screen dimensions of 474 x 297 millimeters and resolution of 1680 x 1050 pixels. Reading task can be considered as an intermediate case between the static and the dynamic stimuli due to the semi-predefined path imposed by the text structure, ensuring the continuous dynamics of the exhibited eye movements and the resulting fixation density map that is more uniformly spaced and less cluttered. We made a point to include this dataset in our experiments in order to assess the amount of information that can be extracted from spatial characteristics of eye movement signals in response to reading. For every recording a fixation density map is constructed and used as a biometric template during the comparison stage.

Video datasets

These datasets were recorded with the same experimental settings used in the previous experiment (for the Text dataset) and with the same large pool of 100 subjects. The average calibration accuracy in this case was 0.48^0 (SD = 0.17^0) and the average recorded data validity 96.16% (SD = 4.41%). The presented stimulus consists of dynamic content. More specifically it includes video scenes from the official trailer of the Hollywood film "Hobbit 2: The Desolation of Smaug (2013)". In order to avoid mental fatigue effects we split the trailer into two parts of one minute each, forming thus two datasets that correspond to the different sections of the trailer, i.e. Video P01 dataset and Video P02 dataset. Each trailer part contains dynamically changing content, including fast action scenes, static scenes with emotional content and briefly presented text banners. With the specific stimulus being a time changing image sequence, the construction of a single fixation density map with the use of all eye positional samples would provide a cluttered (i.e. noisy) for statistical analysis template, due to overlap between multiple recorded samples for the same region during duration of the video. To negate this effect of cluttering each of the recordings is segmented into 2 second intervals and a corresponding fixation density map is built for each of these segments. By comparing the fixation density maps for the segments that correspond to the same time interval and averaging the calculated similarities over them we may construct the similarity matrices which are then fed to the classification module.

3.2 Evaluation of the Biometric Recognition Performance

In this section we will present the identification results demonstrating in parallel to what degree the selected value for the Gaussian standard deviation may influence the performance of the two employed comparison schemes. During the experiments we employed two measures that are commonly used in biometric identification research, the Rank-1 Identification accuracy (IR) and the Equal Error Rate (EER). The Rank-1 Identification accuracy (IR) refers to the rate at which the biometric templates from the subjects of a database are identified as belonging to the correct individual. By varying the acceptance threshold, we can calculate the False Acceptance Rate (FAR), which refers to the rate that the imposter samples are identified as correct and the False Rejection Rate (FRR), which refers to the rate that the genuine samples fail to pass the acceptance threshold. The Equal Error Rate can be defined then as the point to which the False Acceptance Rate equals the False Rejection Rate. In order to calculate the reported identification rates we used the

similarity matrices from the comparison procedure and averaged the results over 20 iterations by applying a 50%-50% (test-train) random split of the samples by subject for every iteration.

In Table 1 we can observe the Rank-1 accuracy for the Similarity metric by varying the value of the Gaussian kernel σ (normalized in map's width) that was used during the construction of the fixation density maps. A close inspection of the results reveals the degree to which the variation of the standard deviation (σ) of the Gaussian kernel can affect the resulting identification accuracies and also that the optimum performances were achieved for a value of σ in the range 0.016-0.032. The maximum IR that can be achieved with the specific comparison measure for the **Faces** dataset is **48.7%**, whereas for the **Video P01** dataset it reaches a **35.5%** and for **Video P02** dataset a **36.8%**. The measure yields very low rates for the **Text** dataset, presenting an IR of **11.9%**.

A remarkable improvement can be observed in performance with the use of KL-divergence as a comparison measure, as demonstrated from the calculated IR values in Table 2. The identification accuracy for the **Faces** dataset peaks to **82.6%** and an analogous improvement is achieved for **Video P01** with an IR of **50.3%** and for **Video P02** with a **52.4%**. The identification rates have increased in the case of the **Text** dataset too - although they are once again the worst among the four sets - reaching a **36.4%**.

Table 1. Rank-1 Identification accuracy (IR) for different values of the Gaussian kernel σ for the Similarity metric.

Similarity metric				
Gaussian σ	**Faces dataset**	**Video P01 dataset**	**Video P02 dataset**	**Text dataset**
0.008	43.0%	20.2%	25.7%	8.6%
0.016	48.3%	35.2%	**36.8%**	8.7%
0.032	**48.7%**	**35.5%**	34.6%	**11.9%**
0.064	42.3%	28.2%	25.7%	9.1%
0.128	36.2%	22.7%	21.1%	4.3%

Table 2. Rank-1 Identification accuracy (IR) for different values of the Gaussian kernel σ for the KL-divergence.

KL-divergence				
Gaussian σ	**Faces dataset**	**Video P01 dataset**	**Video P02 dataset**	**Text dataset**
0.008	76.5%	34.3%	37.3%	33.1%
0.016	78.8%	42.4%	46.7%	**36.4%**
0.032	76.9%	**50.3%**	**52.4%**	35.4%
0.064	**82.6%**	50.0%	48.1%	34.7%
0.128	78.0%	43.7%	46.3%	28.0%

In order to assess the efficacy of the proposed method in a more general framework, we have constructed the corresponding ROC curves for the four employed datasets, both for the Similarity metric and for the KL-divergence measure. The ROC curves depict the False Acceptance Rate in relation to the True Positive Rate (TPR), which is the rate of the genuine samples that are correctly identified (TPR = 1 - FRR). For the construction of these curves we used the optimum values that were determined during the parametric analysis involving the adopted standard deviation (σ) for the Gaussian kernel.

Figure 4 demonstrates the constructed ROC curves for the Similarity metric, from which we may calculate the EER for each of the used datasets. As it may be observed, the achieved EER for the **Faces** dataset presents a relatively high value of **34.5%**, whereas for **Video P01** and **Video P02** datasets the achieved rates present lower values of **29.7%** and **25.9%** accordingly. For the **Text** dataset the EER has a value of **33.2%** which is almost as high as the corresponding rate for the Faces dataset.

As in the case of IR, the KL-divergence measure exhibits superior performance also during the EER calculation. It can be observed in Figure 5 that a considerable improvement is achieved in all cases, with a remarkably lower EER of **22.5**% for the **Faces** dataset, whereas the corresponding EER values for **Video P01**, **Video P02** and **Text datasets** have also been improved considerably to **20.4**%, **18.3**% and **20.4**%.

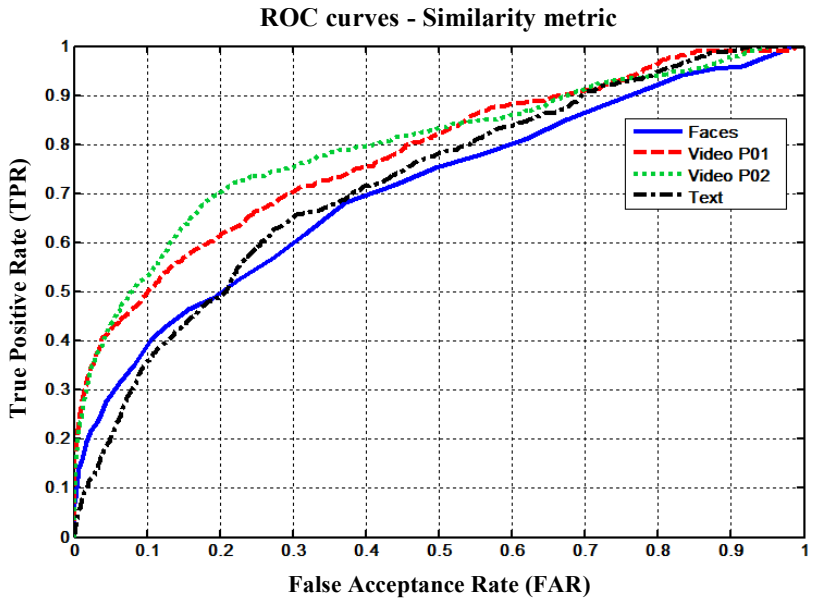

Figure 4. ROC curves for the employed datasets and for the measure of Similarity metric.

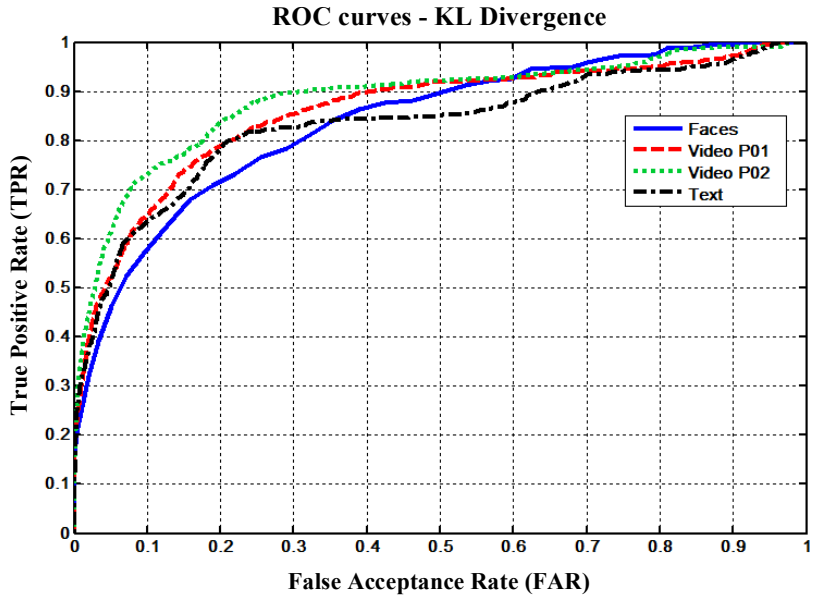

Figure 5. ROC curves for the employed datasets and for the measure of KL-divergence.

4. DISCUSSION

The evaluation procedure unveiled several notable findings. First, the results confirm the ability of the proposed fixation-based biometrics method to extract at a certain degree person specific characteristics that can be used for identification in dynamic visual environments. In addition, the demonstrated performance for the video sequence datasets revealed the capability of the proposed approach to operate in the case of a time changing visual stimulus. However, the method seemed to perform in general with poorer rates in the case of the Text dataset. This inferior performance may be attributed to the fact that the text stimulus, as already mentioned, creates an environment in which the eye movements cannot be considered as absolutely unguided. As a result, a method that might employ time dynamics (e.g. velocity or acceleration characteristics) would probably perform more efficiently for this type of stimulus. Second, regarding the two comparison measures employed for the task of biometrical identification via the proposed biometric feature, the KL-divergence proved to be more effective than Similarity metric on capturing the individual characteristics that may be encapsulated on the formatted biometrical templates. Third, concerning the influence of the Gaussian standard deviation (σ) on the constructed fixation density maps, the parametric analysis revealed that a value in the range of 0.016-0.032 can be globally adopted for achieving relatively adequate identification rates in the vast majority of experimental settings. Finally, it should be highlighted that the achieved EER of 22.5% for the Faces dataset (in the case of KL-divergence) improves on the previously reported rate of 30% in [7], where spatial eye movement features were also employed.

It should be noticed that the nature of the employed datasets imposes certain limitations. Compared to the experiments where a jumping point stimulus is employed, an experiment that includes a free-viewing stimulus is more difficult to be repeated many times due to the involved active visual processing scheme. As a result, the number of samples per subject for the used datasets is relatively low. Furthermore, during the experiments the eye movements were recorded in a controlled environment (e.g. with limited head movement allowed), which will be rarely the case for a real world biometric system. These conditions should be taken into consideration during the inspection of the obtained accuracies in the evaluation process.

5. CONCLUSION & FUTURE WORK

In this paper a novel biometric recognition scheme based on the fixation density map was proposed. The research concerning eye movements on biometrics has been relatively recently established but it has already presented promising results for the exploration of the physical and behavioral traits of an individual. Since most of the work in the field regards features of the spectral domain or time dynamics (velocity, acceleration) but little research has been conducted with the employment of spatial features, we decided to develop a method that is capable to represent the visual scanpath on the stimulus plane and to extract idiosyncratic characteristics for the biometric identification of subjects under free viewing conditions. The identification rates still lack the high accuracy and permanence of the methods that rely on physical cues (fingerprints, iris etc.) but the characteristics extracted from eye movements encapsulate behavioral information, which in turn can be integrated as a complementary biometrical cue in multi-modal systems in order to provide robustness and security enhancement during the identification procedure.

In the future work we are targeting to increase the databases size and number of samples per subject in order to research the scalability of the proposed techniques and also inspect possible optimization schemes for the selection of the parameters (e.g. Gaussian σ, time segmentation interval in the case of dynamic stimuli etc.) during the construction of the fixation density maps. We also expect the proposed method would be more robust to the degradation of the sampling frequency of the recording eye tracking equipment when compared to other eye movement-biometrics methods explored so far.

6. ACKNOWLEDGEMENTS

This work is supported in part by NSF CAREER Grant #CNS-1250718 and NIST Grants #60NANB10D213 and #60NANB12D234. Special gratitude is expressed to Dr. Evgeny Abdulin, Tjitse Miller, Christina Heinich for proctoring eye movement recordings.

REFERENCES

[1] Google. Google Glass. Available: http://www.google.com/glass/start/

[2] Komogortsev, O.V., Holland, C., Karpov, A. and Proença, H., "Multimodal Ocular Biometrics Approach: A Feasibility Study," Proc. IEEE Fifth International Conference on Biometrics: Theory, Applications and Systems (BTAS), 1-8 (2012).

[3] Kasprowski, P. and Ober, J., "Eye movements in Biometrics," Maltoni, D. and Jain, A. (Eds.), LNCS 3087, Biometric Authentication, Springer, Heidelberg, 248-258 (2004).

[4] Bednarik, R., Kinnunen, T., Mihaila, A. and Franti, P., "Eye-Movements as a Biometric," Kalviainen, H., Parkkinen, J. and Kaarna, A., (Eds.), LNCS 3540, Image Analysis, Springer, Heidelberg, 780-789 (2005).

[5] Kinnunen, T., Sedlak, F. and Bednarik, R., "Towards Task-Independent Person Authentication using Eye Movement Signals," Proc. 2010 Symposium on Eye-Tracking Research & Applications (ETRA), New York, USA, 187-190 (2010).

[6] Komogortsev, O.V., Karpov, A., Price, L. and Aragon, C., "Biometric Authentication via Oculomotor Plant Characteristic," Proc. IEEE/IARP International Conference on Biometrics (ICB), 1-8 (2012).

[7] Rigas, I., Economou, G. and Fotopoulos, S., "Biometric identification based on the eye movements and graph matching techniques," Pattern Recognition Letters 33(6), 786-792 (2012).

[8] Holland, C.D. and Komogortsev, O.V., "Complex Eye Movement Pattern Biometrics: The Effects of Environment and Stimulus," IEEE Transactions on Information Forensics and Security 8(12), 2115-2126, (2013).

[9] Komogortsev, O.V. and Holland C.D., "Biometric Authentication via Complex Oculomotor Behavior," Proc. IEEE Sixth International Conference on Biometrics: Theory, Applications and Systems (BTAS), 1-8, (2013).

[10] Itti, L., Koch, C. and Niebur, E., "A Model of Saliency-Based Visual Attention for Rapid Scene Analysis," IEEE Transactions on Pattern Analysis and Machine Intelligence (PAMI) 20(11), 1254-1259 (1998).

[11] Harel, J., Koch, C. and Perona, P., "Graph-Based Visual Saliency," Proc. of Neural Information Processing Systems (NIPS), 2006.

[12] Li, J., Levine, M.D., An, X., Xu, X. and He, H., "Visual Saliency Based on Scale-Space Analysis in the Frequency Domain," IEEE Transactions on Pattern Analysis and Machine Intelligence (PAMI) 35(4), 996-1010 (2013).

[13] Judd, T., Durand, F. and Torralba, A., "A Benchmark of Computational Models of Saliency to Predict Human Fixations," MIT-CSAIL-TR-2012-001, available at: http://hdl.handle.net/1721.1/68590 (2012).

[14] Kullback, S. and Leibler, R.A., "On Information and Sufficiency," Annals of Mathematical Statistics 22(1), 79-86 (1951).

[15] Pekalska, E., Paclik, P. and Duin, R., "A generalized kernel approach to dissimilarity-based classification," Journal of Machine Learning Research 2, 175-211 (2001).

[16] Chen Y., Garcia E.K., Gupta M.R., Rahimi A. and Cazzanti L., "Similarity-based Classification: Concepts and Algorithms," Journal of Machine Learning Research 10, 747-776, (2009).

[17] EyeLink. EyeLink 1000 Eye Tracker. Available: http://www.sr-research.com/